

Efficacy of regularized multi-task learning based on SVM models

Shaohan Chen, Zhou Fang, Sijie Lu, and Chuanhou Gao, *Senior Member, IEEE*

Abstract—This paper investigates the efficacy of a regularized multi-task learning (MTL) framework based on SVM (M-SVM) to answer whether MTL always provides reliable results and how MTL outperforms independent learning. We first find that M-SVM is Bayes risk consistent in the limit of large sample size. This implies that despite the task dissimilarities, M-SVM always produces a reliable decision rule for each task in terms of misclassification error when the data size is large enough. Furthermore, we find that the task-interaction vanishes as the data size goes to infinity, and the convergence rates of M-SVM and its single-task counterpart have the same upper bound. The former suggests that M-SVM cannot improve the limit classifier’s performance; based on the latter, we conjecture that the optimal convergence rate is not improved when the task number is fixed. As a novel insight of MTL, our theoretical and experimental results achieved an excellent agreement that the benefit of the MTL methods lies in the improvement of the pre-convergence-rate factor (PCR, to be denoted in Section III) rather than the convergence rate. Moreover, this improvement of PCR factors is more significant when the data size is small.

Index Terms—Multi-task learning, error analysis, learning theory, regularization method, pre-convergence-rate factor.

I. INTRODUCTION

RECENT years have seen a considerable success of machine learning technologies, including deep neural networks (DNNs), SVMs, decision trees, etc. These methods usually work well when the training and test data are drawn from the same distribution and “big data” is available (e.g., DNNs). However, the conditions of the same distribution and “big data” cannot always hold in many real-world problems—for example, building self-driving systems and modeling rare diseases in healthcare records. Thus, developing methods to learn multiple tasks simultaneously and efficiently is significant. In this case, multi-task learning (MTL) [1] provides a general way to accommodate these situations. A vast of elaborate MTL methods have been designed in various settings to solve specific problems [2]–[11].

Also, there have been a lot of notable theoretical justifications for the superiority of MTL over independent learning. Ando et al. [12] studied MTL based on structural learning and showed that it estimates the shared hypothesis space more reliably if the number of tasks T is large enough. Baxter [13],

[14] investigated MTL in the framework of bias learning and showed that it significantly reduces the sampling burden for good generalization on novel tasks if T is arbitrarily large. He also illustrated that MTL (within a Bayesian context) efficiently decays the information required to learn each task as T grows considerably [15]. Maurer et. al. [16] discussed MTL in representation learning and showed that it vanishes the cost to learn the representation in the multi-task limit ($T \rightarrow \infty$). Liu et. al. [17] analyzed MTL using the sample average stability measure and showed that it estimates the shared parameter more accurately when T is large enough. Zhao et. al. [18] viewed MTL as a vector-valued function learning problem and showed that it requires a smaller sample size of each task to achieve the same performance.

The existing theoretical analysis of MTL relies on the pursuit of tighter error bounds, which is not enough to guarantee the superiority of MTL. Moreover, as introduced above, the advantages of MTL can so far only be seen when T is sufficiently large, which makes MTL challenging to be trusted by users. The arbitrarily large T requirement is rarely satisfied in real applications, e.g., it is often difficult to access a dataset with large T in the healthcare and industrial systems. Therefore, it is crucial to investigate the intrinsic benefits of MTL by applying a more elaborate analysis method to it when T is fixed.

This paper moves the steps forward and tries to explore the essential benefits of MTL with respect to the misclassification error when T is fixed. Particularly, we concern with a popular regularized multi-task SVM (M-SVM) proposed by [19], which provides an avenue to share useful knowledge among tasks through parameters. Note that the analysis of the misclassification error has been intensively researched in the single-task learning contexts [20]–[25]. This work solved two main technical difficulties of adapting the misclassification error analysis to MTL: considering the interactions between tasks carefully and estimating the additional error caused by the randomness of the sampling frequencies for each task (see Section III).

We first analyze the asymptotic performance of M-SVM to show that it is Bayes risk consistent in the limit of large sample size. This implies that despite the task dissimilarities, M-SVM always produces a reliable decision rule for each task in terms of the misclassification error when the data size is large enough. Second, we find that the task-interaction vanishes as the data size goes to infinity, and the convergence rates of M-SVM and its single-task counterpart have the same upper bound. The former suggests that M-SVM cannot improve the limit classifier’s performance; based on the latter, we conjecture

This work was supported by the National Natural Science Foundation of China under grants 62111530247 and 12071428, and the Zhejiang Provincial Natural Science Foundation of China under grant LZ20A010002.

S. Chen, S. Lu and C. Gao are with the School of Mathematical Sciences, Zhejiang University, Hangzhou 310027, China (Corresponding e-mail: gaouchou@zju.edu.cn (C. Gao)).

Z. Fang is with the Department of Biosystems Science and Engineering, ETH Zurich, Switzerland.

that the optimal convergence rate is not improved when the number of tasks is fixed. The intuition of this conjecture is that the generalization capacity mainly depends on the hypothesis space's complexity which MTL cannot change.

As a novel insight of MTL, our theoretical (on a one-dimensional classification problem) and experimental results achieved an excellent agreement that the benefit of M-SVM lies in improving the pre-convergence-rate (PCR) factor (which is denoted as the ratio between the excess misclassification error and its real convergence rate in Section III) rather than the convergence rate. Moreover, our simulation results of several other MTL methods, including L21, Lasso, and SRMTL (these models can be found and solved by [26]) also demonstrate the generality of this new insight in MTL. As shown in Section IV-A, the PCR factor is a function of data size, the similarity of the tasks, and regularization parameters, meaning that MTL can achieve a better performance when there exists a good balance of these quantities. Particularly, the improvement of PCR factors in MTL is more significant when the data size is small. To conclude, PCR factor is more suitable and accurate to depict the essential advantages of MTL when T is fixed.

The rest of this paper is organized as follows. Section II introduced the basic notations of MTL and an extension of M-SVM. Section III provided an asymptotic analysis of M-SVM in the limit of large sample size, based on which we raise the main conjecture in this paper. In Section IV, both the theoretical and experimental analysis were provided to verify the correctness of our conclusions. Section V presented several discussions, and Section VI concluded this paper. To improve the readability of this paper, we put all proofs in the appendix.

II. METHOD

A. Problem settings and notations

We consider the following MTL setting. Assume we are facing T learning tasks and samples for each task comes out randomly with probability $p(t)$ at each time, for $t = 1, \dots, T$. After a short time, we collect N data points totally from T tasks and suppose that all these samples belonging to the same space $X \times Y$, where $X \subset \mathbb{R}^d$ and $Y = \{-1, 1\}$. Specifically, for each task t , there are m_t samples generated from the distribution $P_t(\mathcal{X}, \mathcal{Y})$, for $t = 1, \dots, T$. That is,

$$\left\{ \{(\mathbf{x}_{11}, y_{11}), \dots, (\mathbf{x}_{m_1 1}, y_{m_1 1})\}, \dots, \{(\mathbf{x}_{1T}, y_{1T}), \dots, (\mathbf{x}_{m_T T}, y_{m_T T})\} \right\}. \quad (1)$$

For better adapting to the real scenarios, we assume $p(t)$ is different from each task, while their distribution functions $P_t(\mathcal{X}, \mathcal{Y})$ are closely related. The ideal goal of MTL is to learn T functions simultaneously f_1, \dots, f_T such that $\text{sgn}(f_t)(\mathbf{x}_{it}) = y_{it}$, for $i = 1, \dots, m_t$, $t = 1, \dots, T$.

Based on the above settings, we define the average misclassification error for these T classifiers to be the weighted sum of the corresponding misclassification errors [20]: $\mathcal{U}(\text{sgn}(f_1), \dots, \text{sgn}(f_T)) = \sum_{t=1}^T p(t) \mathcal{R}_t(\text{sgn}(f_t))$, where $\mathcal{R}_t(f_t) = \mathbb{E}_{\mathcal{X}, \mathcal{Y}} \mathbf{1}(\text{sgn}(f_t)(\mathcal{X}) \neq \mathcal{Y})$, for $t = 1, \dots, T$, and $\mathbf{1}(A)$ is an indicator function with its value being one if the event A is true, and zero if it is not. We see that the average

misclassification error actually measures the risk of applying f_1, \dots, f_T to make predictions.

We define the minimizer of the misclassification error for each task as $f_t^* = \arg \inf_{f_t} \mathcal{R}_t(f_t)$, where the infimum is over all measurable functions. Based on [27], this minimizer has the expression as $f_t^*(x) = \text{sgn}(\eta_t(x) - \frac{1}{2})$ and is called Bayes rule, where $\eta_t(x) = P_t(\mathcal{Y} = 1 | \mathcal{X} = x)$, for $t = 1, \dots, T$.

We now define the average expected error of T function f_1, \dots, f_T with respect to a loss function $\ell: \mathbb{R} \rightarrow [0, \infty)$ as $\mathcal{E}(f_1, \dots, f_T) = \sum_{t=1}^T p(t) \mathbb{E}_{(\mathcal{X}, \mathcal{Y}) \sim P_t} [\ell(\mathcal{Y} f_t(\mathcal{X}))]$, then the corresponding average empirical error is $\mathcal{E}_z(f_1, \dots, f_T) = \sum_{t=1}^T \sum_{i=1}^{m_t} \frac{1}{N} \ell(y_{it} f_t(\mathbf{x}_{it}))$.

This paper mainly concerns with the following denotations. For each task t , we define the **excess misclassification error** of the classifier $\text{sgn}(f_t)$ as $\mathcal{R}(\text{sgn}(f_t)) - \mathcal{R}(f_t^*)$. For all the T tasks, the **average excess misclassification error** of the classifiers $\text{sgn}(f_t)$ ($t = 1, \dots, T$) is defined as $\mathcal{U}(\text{sgn}(f_1), \dots, \text{sgn}(f_T)) - \mathcal{U}(f_1^*, \dots, f_T^*)$, and the **average excess expected error** of the functions f_t ($t = 1, \dots, T$) is defined as $\mathcal{E}(f_1, \dots, f_T) - \mathcal{E}(f_1^*, \dots, f_T^*)$.

B. M-SVM method

This section extends M-SVM originating from [19] to a more general case, where we assume that the functions f_1, \dots, f_T are nonlinear and the probability of each sample coming out from task t is $p(t)$ instead of $\frac{1}{T}$. Notice that the exact $p(t)$ is generally unknown, we use the sampling frequency $\frac{m_t}{N}$ to approximate $p(t)$ for each task in the problem and obtain an extend version of M-SVM as follows,

$$\begin{aligned} \min_{\substack{f_0, f_1, \dots, f_T \in \mathcal{H}_K \\ \xi_{it} \in \mathbb{R}}} & \left\{ \sum_{t=1}^T \sum_{i=1}^{m_t} \xi_{it} + \lambda_1 \sum_{t=1}^T \frac{m_t}{N} \|g_t\|_K^2 \right. \\ & \left. + \lambda_2 \|f_0\|_K^2 \right\} \\ \text{s.t.} & y_{it} \cdot f_t(\mathbf{x}_{it}) \geq 1 - \xi_{it}, \quad \xi_{it} \geq 0, \\ & i = 1, \dots, m_t; \quad t = 1, \dots, T. \end{aligned} \quad (2)$$

where λ_1 and λ_2 are two positive regularization parameters, K is a universal kernel (e.g, the Gaussian kernel), \mathcal{H}_K is the Reproducing Kernel Hilbert Space (RKHS) [20], $\|\cdot\|_K$ is the norm function in this Hilbert space, and $g_t := f_t - f_0$. Since (2) contains regularization terms $\|g_t\|_K^2$ and $\|f_0\|_K^2$ that models task relations, we refer this as a regularized MTL model. In Eq. (2), f_0 represents the commonness of those classifiers, while g_t , $t = 1, \dots, T$, represent their individualities. The extended model of (2) will be reduced to the original one [19] when m_t ($t = 1, \dots, T$) are identical. Note that considering the randomness in the sampling frequency for each task makes the proposed method better adaptable to real applications, as the model pays more attention to the higher frequency tasks. Hence, the M-SVM Eq. (2) well extends the original MTL framework. By the positive definiteness and convexity of the loss function and the norm function, there exists the optimal solution of (2).

Following the similar calculation scheme of [19], and denoting f_t^z ($t = 1, \dots, T$), f_0^z to be the optimal solution of Eq. (2), we can get a relation of these quantities in Lemma 1, and then reformulate Eq. (2) as Eq. (3) in Theorem 1.

Lemma 1 (Adapted from [19, Lemma 2.1]). *The optimal solution to the Eq. (2) satisfies the equation $f_0^z = \frac{\lambda_1}{\lambda_2 + \lambda_1} \sum_{t=1}^T \frac{m_t}{N} f_t^z$.*

Theorem 1 (Adapted from [19, Lemma 2.2]). *The multi-task problem Eq. (2) is equivalent to the optimization problem below:*

$$\begin{aligned} \min_{\substack{f_1, \dots, f_T \in \mathcal{H}_K \\ \xi_{it} \in \mathbb{R}}} & \left\{ \sum_{t=1}^T \sum_{i=1}^{m_t} \xi_{it} + \rho_1 \sum_{t=1}^T \frac{m_t}{N} \|f_t\|_K^2 \right. \\ & \left. + \rho_2 \sum_{t=1}^T \frac{m_t}{N} \left\| f_t - \sum_{s=1}^T \frac{m_s}{N} f_s \right\|_K^2 \right\} \quad (3) \\ \text{s.t.} & \quad y_{it} \cdot f_t(\mathbf{x}_{it}) \geq 1 - \xi_{it}, \quad \xi_{it} \geq 0, \\ & \quad i = 1, \dots, m_t; \quad t = 1, \dots, T. \end{aligned}$$

where $\rho_1 = \frac{\lambda_1 \lambda_2}{\lambda_1 + \lambda_2}$ and $\rho_2 = \frac{\lambda_1^2}{\lambda_1 + \lambda_2}$.

Theorem 1 indicates that M-SVM works by achieving a good trade-off between independent learning (i.e., the second term in (3)) and aggregate learning that treats different tasks as the one (i.e., the last term in (3)).

In the next section, we will show an asymptotic property of M-SVM in Eq. (3) that it is Bayes risk consistent in the limit of large sample size.

III. ASYMPTOTIC PERFORMANCE OF M-SVM

In this section, we first present the average excess misclassification error bound for M-SVM (3). Then, based on the analysis of this bound, we raise the main conjecture that the superiority of M-SVM is the improvement of the PCR factor rather than the convergence rate.

A. Error analysis of M-SVM

This subsection derives an upper bound of the average excess misclassification error for M-SVM (3): $\mathcal{U}(\text{sgn}(f_1^z), \dots, \text{sgn}(f_T^z)) - \mathcal{U}(f_1^*, \dots, f_T^*)$, by extending the analysis techniques for the single-task setting [20], [21], [25], [28], [29]. The definition of this error is given in Section II-A.

First, we show the minimizers of the average expected error $\mathcal{E}(f_1, \dots, f_T)$ to be the Bayes rules.

Theorem 2. *The minimizers of $\mathcal{E}(f_1, \dots, f_T)$ over all measurable functions are the Bayes rules f_t^* , where $t = 1, \dots, T$.*

Proof. Note that the minimizer of each $\mathbb{E}_{(\mathcal{X}, \mathcal{Y}) \sim P_t} [\ell(\mathcal{Y} f_t(\mathcal{X}))]$ is the Bayes rule f_t^* over all measurable functions [30, lemma 3.1]. By the definition, the Bayes rules also minimize $\mathcal{E}(f_1, \dots, f_T)$. \square

Theorem 2 implies one advantage of the MTL framework of (3) that it leverages the related tasks by introducing a regularization term in the objective function without imposing the additional restrictions on the functional space [12], [16], and, therefore, the best rule (Bayes rule) is not precluded.

Similar to the single-task case, there exists a bridge inequality which connects the average excess misclassification error with the average excess expected error.

Theorem 3. *For any $h_t : X \rightarrow \mathbb{R}, t = 1, \dots, T$, there exists a bridge inequality between the average misclassification error $\mathcal{U}(h_1, \dots, h_T)$ and the average expected error $\mathcal{E}(h_1, \dots, h_T)$:*

$$\begin{aligned} & \mathcal{U}(\text{sgn}(h_1), \dots, \text{sgn}(h_T)) - \mathcal{U}(f_1^*, \dots, f_T^*) \\ & \leq \mathcal{E}(h_1, \dots, h_T) - \mathcal{E}(f_1^*, \dots, f_T^*). \end{aligned} \quad (4)$$

Proof. Notice that for each $h_t : X \rightarrow \mathbb{R}$ the inequality $\mathcal{R}_t(\text{sgn}(h_t)) - \mathcal{R}_t(f_t^*) \leq \mathcal{E}_t(h_t) - \mathcal{E}_t(f_t^*)$ has established in [31], where $\mathcal{E}_t(h_t) = \mathbb{E}_{(\mathcal{X}, \mathcal{Y}) \sim P_t} [\ell(\mathcal{Y} h_t(\mathcal{X}))]$. Then by the definitions of $\mathcal{U}(h_1, \dots, h_T)$ and $\mathcal{E}(h_1, \dots, h_T)$, we can get the desired result directly. \square

Let $(f_1^{\mathcal{H}}, \dots, f_T^{\mathcal{H}})$ be the minimizer of the average expected error over the RKHS space $\prod_{t=1}^T \mathcal{H}_K$, i.e.,

$$\begin{aligned} (f_1^{\mathcal{H}}, \dots, f_T^{\mathcal{H}}) &= \underset{h_1, \dots, h_T \in \mathcal{H}_K}{\text{argmin}} \left\{ \mathcal{E}(h_1, \dots, h_T) \right. \\ & \left. + \frac{\rho_1}{N} \sum_{t=1}^T p(t) \|h_t\|_K^2 + \frac{\rho_2}{N} \sum_{t=1}^T p(t) \left\| h_t - \sum_{s=1}^T p(s) h_s \right\|_K^2 \right\}, \end{aligned}$$

where the existence of $(f_1^{\mathcal{H}}, \dots, f_T^{\mathcal{H}})$ is guaranteed by the positive definiteness and convexity of the loss function and the norm function. Then we have the following lemma, which gives an upper bound of the average excess expected error.

Lemma 2. *The following inequality holds:*

$$\begin{aligned} & \mathcal{E}(f_1^z, \dots, f_T^z) - \mathcal{E}(f_1^*, \dots, f_T^*) \\ & \leq \mathcal{S}(N, T) + \mathcal{D}(N, T, \rho_1, \rho_2) + \mathcal{F}(N, T, \rho_1, \rho_2) \end{aligned}$$

where

$$\begin{aligned} \mathcal{S}(N, T) &:= \{ \mathcal{E}(f_1^z, \dots, f_T^z) - \mathcal{E}_z(f_1^z, \dots, f_T^z) \} \\ & \quad + \{ \mathcal{E}_z(f_1^{\mathcal{H}}, \dots, f_T^{\mathcal{H}}) - \mathcal{E}(f_1^{\mathcal{H}}, \dots, f_T^{\mathcal{H}}) \}, \end{aligned}$$

$$\begin{aligned} \mathcal{D}(N, T, \rho_1, \rho_2) &:= \inf_{h_1, \dots, h_T \in \mathcal{H}_K} \left\{ [\mathcal{E}(h_1, \dots, h_T) \right. \\ & \quad \left. - \mathcal{E}(f_1^*, \dots, f_T^*)] + \frac{\rho_1}{N} \sum_{t=1}^T p(t) \|h_t\|_K^2 \right. \\ & \quad \left. + \frac{\rho_2}{N} \sum_{t=1}^T p(t) \left\| h_t - \sum_{s=1}^T p(s) h_s \right\|_K^2 \right\}, \end{aligned}$$

and

$$\begin{aligned} \mathcal{F}(N, T, \rho_1, \rho_2) &= -\frac{\rho_1}{N} \sum_{t=1}^T \left(p(t) - \frac{m_t}{N} \right) \|f_t^{\mathcal{H}}\|_K^2 \\ & \quad + \frac{\rho_2}{N} \sum_{t=1}^T \left(\frac{m_t}{N} - p(t) \right) \left\| f_t^{\mathcal{H}} - \sum_{s=1}^T \frac{m_s}{N} f_s^{\mathcal{H}} \right\|_K^2 \\ & \quad + \frac{2\rho_2}{N} \sum_{t=1}^T p(t) \left\| f_t^{\mathcal{H}} - \sum_{s=1}^T \frac{m_s}{N} f_s^{\mathcal{H}} \right\|_K \left\| \sum_{t=1}^T \left(p(t) - \frac{m_t}{N} \right) f_t^{\mathcal{H}} \right\|_K \end{aligned}$$

The proof of Lemma 2 can be found in the appendix.

Similar to [20], we refer to the first term $\mathcal{S}(N, T)$ as the average sample error and the second term $\mathcal{D}(N, T, \rho_1, \rho_2)$ as the average regularization error. It is worth to notice that we have an additional term $\mathcal{F}(N, T, \rho_1, \rho_2)$ in Lemma 2, compared to literature [20]. Here we refer to it as the frequency

error, because one of its dominant term, $p(t) - \frac{m_t}{N}$, measures the sampling frequency error of each task. The frequency error vanishes in the single-task learning cases where the sampling frequency is deterministic, i.e. $m_1 = N$. Therefore, the frequency error is a new knowledge associated with the MTL problems only.

To bound these three errors, we have the following lemmas.

Lemma 3. *An upper bound of the average sample error can be given by $\mathcal{S}(N, T) = \mathcal{O}(N^{-1/4+\epsilon})$ almost surely, where ϵ is any positive constant.*

Lemma 4. *Assume that the Bayes rules for each task f_t^* ($t = 1, \dots, T$) are restrictions of some functions \tilde{f}_t^* lying in the Sobolev space $H^s(\mathcal{R}^d)$. Then, an upper bound of the average regularization error can be given by $\mathcal{D}(N, T, \rho_1, \rho_2) = \mathcal{O}((\log N)^{-s/4})$ almost surely.*

Lemma 5. *An upper bound of the frequency error can be given by $\mathcal{F}(N, T, \rho_1, \rho_2) = \mathcal{O}(N^{-3/2+\epsilon})$ almost surely, where ϵ is any positive constant.*

The proof of Lemmas 3, 4 and 5 can be found in the appendix.

Combining the results of Theorem 3, Lemmas 2, 3, 4 and 5, we can provide the main result of this section in the theorem below.

Theorem 4. *Assume that f_t^* ($t = 1, \dots, T$) are the restrictions of some functions \tilde{f}_t^* lying in the Sobolev space $H^s(\mathcal{R}^d)$. Then, an upper bound of excess average misclassification error can be obtained almost surely by*

$$\mathcal{U}(\text{sgn}(f_1^z), \dots, \text{sgn}(f_T^z)) - \mathcal{U}(f_1^*, \dots, f_T^*) = \mathcal{O}((\log N)^{-s/4}). \quad (5)$$

Proof. It follows from Theorem 3, Lemmas 2, 3, 4 and 5. \square

Corollary. *Almost surely, the misclassification error $\mathcal{R}_t(f_t^z)$ for each task t , ($t = 1, \dots, T$), can be arbitrarily close to the corresponding Bayes error $\mathcal{R}_t(f_t^*)$, as long as N is sufficiently large.*

Theorem 4 indicates that the average misclassification error $\mathcal{U}(\text{sgn}(f_1^z), \dots, \text{sgn}(f_T^z))$ can be arbitrarily close to the average Bayes error $\mathcal{U}(f_1^*, \dots, f_T^*)$, as long as N is sufficiently large. Moreover, the Corollary above shows that the learned classifier $\text{sgn}(f_t^z)$ for each task t converges to the corresponding Bayes rule f_t^* , when N increases to infinity. Therefore, given a large data size, the M-SVM (3) induces a reliable classification rule for each task with a small misclassification error, which gives us great confidence in this method.

B. Important remarks

1) *Task-interaction vanishes in the limit of large sample size:* Previous literature has shown the Bayes risk consistency of the single-task SVM [20]. Based on this fact, our main result in Theorem 4 implies that applying the M-SVM (3) amounts to learning T tasks independently, when the number of samples is sufficiently large. With this regard, in the MTL framework, the interaction between different tasks vanishes as the sample size

grows greatly. Intuitively, we can observe this point through the objection function of M-SVM (3), that the empirical loss dominates the regularization terms (i.e., the task-interaction terms) when the data size is large; therefore, the influence of the task interaction vanishes in the limit of large sample size. This result implies that when the data size is large enough, M-SVM (3) still makes the reliable decisions even if the tasks considered are significantly deviated from each other. This is quite different from the one in finite sample cases, where the task interaction cannot be negligible and plays a key role in improving the performance of each task. Moreover, as shown in section IV-B and Section IV-C, the performance curves of M-SVM and its single-task counterpart on the simulated and real datasets are initially separable and finally overlap, which supports this point again.

2) *Regularization terms are necessary:* Note that the average regularization error $\mathcal{D}(N, T, \rho_1, \rho_2)$ disappears if $\rho_1 = \rho_2 = 0$. In this case, by the results of Lemma 2, 3, 4, and 5, it seems that a faster convergent rate $\mathcal{O}(N^{-\frac{1}{4}+\epsilon})$ determined by average sample error can be achieved. However, it is not the case. When $\rho_1 = \rho_2 = 0$, we will lose the upper bound estimation of $\|f_t^z\|_K$ (c.f. lemma A.6 in the appendix) and, therefore, fail to analyze the average sample error. To the best of our knowledge, there has been no literature succeed in estimating the sample error without the boundedness of $\|f_t^z\|_K$. In this regard, regularization terms are necessary. In general, the average excess misclassification error bounds are determined by the complexity of the RKHS [20], [23], [32], [33]. Our experimental results in Section IV-B and Section IV-C also show that, without the regularization term, the M-SVM classifier $\text{sgn}(f_t^z)$ for each task cannot converge to the corresponding Bayes rule f_t^* . Therefore, it is important to include the regularization term in MTL.

3) *What benefits does the M-SVM bring?:* Remark III-B1 has shown the equivalence of the M-SVM and its single-task counterpart in terms of their limit classifiers' performance. Meanwhile, both methods' convergence rates have the same upper bound ($\mathcal{O}(\log N)^{-s/4}$) (see Theorem 4 and [20]) determined by the complexity of the RKHS. Though obtaining the optimal convergence rate requires more elaborate analysis of the RKHS [20], we conjecture that both methods' convergence rate are the same when the number of tasks is fixed, as the more elaborate analysis should be applicable for both cases. Consequently, we conjecture that the benefit of M-SVM is the improvement of its pre-convergence-rate (PCR) factor for each task, defined by $C_M(m_t) = \frac{\mathcal{R}(\text{sgn}(f_t^z)) - \mathcal{R}(f_t^*)}{F(m_t)}$, where $1/F(m_t)$ is the M-SVM's exact convergence rate with $F(m_t) \rightarrow \infty$ ($m_t \rightarrow \infty$). Similarly, for each task, we define the PCR factor of SVM and denote it by $C_S(m_t)$. The following section gives the theoretical (in a one-dimensional least-square classification setting) and experimental justifications of this important claim. Our results demonstrate that, in the similar (non-similar)-task setting, there holds $C_M(m_t) < C_S(m_t)$ ($C_M(m_t) > C_S(m_t)$) when m_t is relatively small, and $C_M(m_t) - C_S(m_t) = 0$ as $m_t \rightarrow \infty$.

IV. CASE STUDIES

This section contains three case studies to verify our claims in Section III-B. Specifically, we first provide a theoretical

verification of the improvement of the PCR factor for MTL in a one-dimensional least-square classification setting. Then, we provide the empirical results of the MTL models, including M-SVM (with linear and Gaussian kernels), unregularized M-SVM, L21, LASSO, and SRMTL (the later three models can be found and solved by [26]) on the simulated data. Finally, we conduct experiments on the blast furnace dataset using the M-SVM and its unregularized version with linear kernel. The simulated and experimental results achieve an excellent agreement with the claims in Section III-B. Without loss of generality, we only consider MTL with two tasks and display its performance for the first task (we can obtain a similar result for the second task cause MTL treats both tasks equally).

A. A theoretical justification of PCR factor

This subsection provides a theoretical guarantee of the PCR factor's improvement in MTL on a one-dimensional classification problem. Explicitly, we analyze the ability of MTL originating from [19] based on the least-square classifiers due to its availability of the analytic solution.

We assume that data are sampled from a two-class Gaussian model with $x_1|(y_1 = 1) \sim \mathcal{N}(\mu_1^+, \sigma_1^2)$, $x_1|(y_1 = -1) \sim \mathcal{N}(\mu_1^-, \sigma_1^2)$ for the first task, and $x_2|(y_2 = 1) \sim \mathcal{N}(\mu_2^+, \sigma_2^2)$, $x_2|(y_2 = -1) \sim \mathcal{N}(\mu_2^-, \sigma_2^2)$ for the second task. For each task, we assume there exists no sampling bias of the positive and negative classes. We also assume $\mu_1^+ > \mu_1^-$ and denote $\delta^+ = \mu_2^+ - \mu_1^+$, $\delta^- = \mu_2^- - \mu_1^-$. Based on the problem setting above, the decision boundaries for these two tasks can be expressed as $w_1x + b_1 = 0$ and $w_2x + b_2 = 0$, respectively. Without loss of generality, we can further suppose $w_1 = w_2$, where w_1 and w_2 are two binary variables and only take two values -1 or 1 (will be shown later).

Combining the MTL [19] with the least-square classifiers can naturally produce the multi-task least-square classification model (referred to as ‘‘M-LSC’’) in one-dimensional setting as follows,

$$\min_{b_0, b_1, b_2, w_1, w_2} \left\{ \sum_{t=1}^2 \sum_{i=1}^{m_t} (y_t^i - w_t x_t^i - b_t)^2 + \frac{\lambda_1}{2} \sum_{t=1}^2 w_t^2 \right\},$$

where $b_1 = b_0 + v_1$ and $b_2 = b_0 + v_2$ are two parameters of the decision boundaries for the M-LSC classifiers.

By the method of Lagrange multipliers and the assumption that $w_1 = w_2$, we can easily obtain the optimal solution of the M-LSC problem for the first task as: $b_1^* = \frac{(G-1)}{m_1} \sum_{i=1}^{m_1} w_1^* x_1^i + \frac{G}{m_2} \sum_{i=1}^{m_2} w_2^* x_2^i$, where $w_1^* = w_2^* = \text{sgn} \left(\sum_{t,i} (x_t^i)^+ - \sum_{t,i} (x_t^i)^- \right)$, and $G = \frac{\lambda_1 m_1}{4m_1 m_2 + \lambda_1 (m_1 + m_2)}$. Then, by the definition of Bayes classifier and the problem setting above, we can also get the Bayes classifier for the first task as $f_1^* = \text{sgn} \left(x - \frac{\mu_1^+ + \mu_1^-}{2} \right)$.

Based on the results above, we can now estimate the excess misclassification error for the M-LSC estimate with respect to the first task $f_1 = \text{sgn}(w_1^*(x - x^0))$, where $x^0 = \frac{-b_1^*}{w_1^*}$. As will be shown below, we only need to estimate the MSE of x^0 .

Note that, for the fixed x^0 and w_1^* , there holds $\mathcal{R}(\text{sgn}(f_1)) = \frac{1}{2} (1 - w_1^* [\phi(x^0 - \mu_1^-) - \phi(x^0 - \mu_1^+)])$, where $\phi(\cdot)$ is the

CDF of the standard Gaussian distribution. Then, we have $\mathcal{R}(\text{sgn}(f_1^*)) = \frac{1}{2} (1 - [\phi(\frac{\mu_1^+ - \mu_1^-}{2}) - \phi(\frac{\mu_1^- - \mu_1^+}{2})])$. By Taylor's theorem, and denote $h = x^0 - \frac{\mu_1^- + \mu_1^+}{2}$, we can check that for the x^0 and w_1^* learned by M-LSC, there holds

$$\mathcal{R}(\text{sgn}(f_1)) - \mathcal{R}(\text{sgn}(f_1^*)) = D \cdot \mathbb{E}(h)^2 + \mathcal{O}(\mathbb{E}(h)^4), \quad (6)$$

where $D = [\phi''(\frac{\mu_1^- - \mu_1^+}{2}) - \phi''(\frac{\mu_1^+ - \mu_1^-}{2})] / 4$ is a constant.

By some standard calculations, we can obtain that

$$\mathbb{E}(h)^2 = \frac{(1-G)^2 \sigma_1^2}{m_1} + \frac{G^2 \delta_1^2}{4} + \frac{G^2 \sigma_2^2}{m_2}, \quad (7)$$

where $\delta = \delta^+ + \delta^-$ is the task dissimilarity. Notice that we can degenerate M-LSC results to its single-task counterpart (S-LSC) by making $\lambda_1 = 0$. Then, we see that the real convergence rates of M-LSC and S-LSC are both $\mathcal{O}(\frac{1}{m})$ by assuming $m_1 = m_2 = m$. According to the PCR factor's definition in Section III-B3, the PCR factor of M-LSC is $(1-G)^2 \sigma_1^2 + G^2 \sigma_2^2 + G^2 \delta_1^2 / 4$, and σ_1^2 for the S-LSC case. We describe the PCR factor as a function of data size in Figure 1.

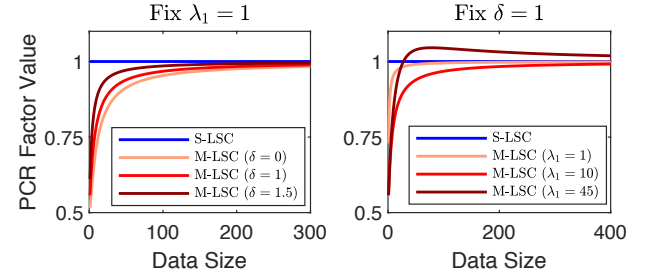


Fig. 1: The change of the PCR factor with the data size m , regularization parameter λ_1 , and task dissimilarity δ . Here, $\sigma_1 = \sigma_2 = 1$, and $m_1 = m_2 = m$.

Our theoretical analysis above demonstrates that PCR factors are different in S-LSC and M-LSC cases. As shown in Figure 1, M-LSC has a smaller PCR factor value when the data size is relatively small, whereas its PCR factor value converges to that of the S-LSC as $m \rightarrow \infty$. This shows that the priority of M-LSC lies in reducing the PCR factor when the data size is relatively small. Furthermore, the PCR factor also depends on the task dissimilarity δ (see the left panel of Figure 1); the less δ is, the less the PCR factor will be. This occurs because more similar tasks contain more common knowledge that can be shared between tasks. Moreover, the PCR factor is related to the regularization parameter λ_1 (see the right panel of Figure 1); particularly, M-LSC can be worse than S-LSC when λ_1 is not properly chosen. Therefore, the capacity of MTL also relies on the choice of tuning parameters.

We theoretically verified that in this case study, the benefit of MTL lies in the improvement of the PCR factor rather than the convergence rate. In what follows, our experiments on the simulated and real data sets demonstrate that this conclusion universally holds in general MTL frameworks.

B. Simulation studies

In this subsection, we first design two simulation studies of M-SVM (one with Gaussian (set its width as 1) and one with

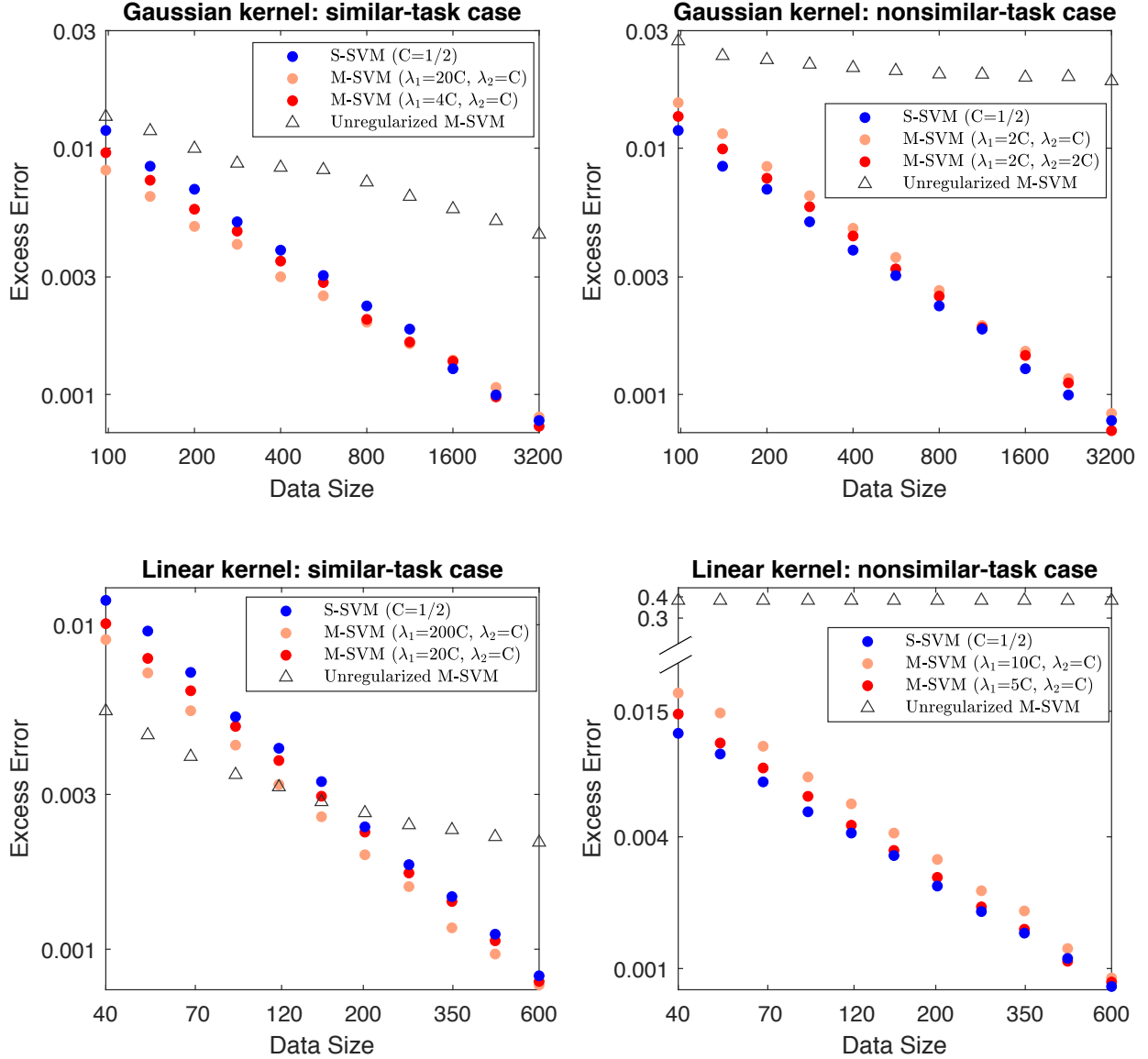


Fig. 2: This figure shows the log-log plot of the excess misclassification error (excess error) to the training data size on the simulated dataset using the S-SVM (with the regularization parameter $C = 1/2$), M-SVM, and unregularized M-SVM in the presence of the randomness in the sampling frequency. For rigorous comparisons, we fixed one of the regularization parameters ($\lambda_1 = 2C$ or $\lambda_2 = C$) for the M-SVM in each case to make it comparable with the S-SVM. The plots of these two models are parallel initially, then get closer gradually and overlap finally, indicating that they have the same convergence rate but different PCR factors. Without the regularization terms, the unregularized M-SVM classifier cannot converge to the corresponding Bayes rule.

linear kernels) to support our claims in Section III-B under two different task dissimilarity settings. To mimic the scenarios in real problems, the data are generated from multi-variate distributions and linearly non-separable, and the uncertainty of the data frequency is also considered. Then, we show that the simulation results of several other MTL methods including L21, LASSO, and SRMTL (these models can be found and solved by [26]) are also consistent with the claims.

For the similar-task setting, we generate data for the first task from a two-class Gaussian model with $\mathbf{x}_1|(y_1 = 1) \sim \mathcal{N}(\begin{bmatrix} 2 \\ 3 \end{bmatrix}, \begin{bmatrix} 1 & 0 \\ 0 & 2 \end{bmatrix})$, $\mathbf{x}_1|(y_1 = -1) \sim \mathcal{N}(\begin{bmatrix} 4 \\ 5 \end{bmatrix}, \begin{bmatrix} 1 & 0 \\ 0 & 2 \end{bmatrix})$. We generate data for the second task from the other two-class Gaussian

model with $\mathbf{x}_2|(y_2 = 1) \sim \mathcal{N}(\begin{bmatrix} 2.2 \\ 3.2 \end{bmatrix}, \begin{bmatrix} 1 & 0 \\ 0 & 2 \end{bmatrix})$, $\mathbf{x}_2|(y_2 = -1) \sim \mathcal{N}(\begin{bmatrix} 4.0 \\ 5.4 \end{bmatrix}, \begin{bmatrix} 1 & 0 \\ 0 & 2 \end{bmatrix})$. For the nonsimilar-task case, we generate data for the first task the same as the above, while we assume data for the second task are sampled from $\tilde{\mathbf{x}}_2|(\tilde{y}_2 = 1) \sim \mathcal{N}(\begin{bmatrix} 7 \\ 8 \end{bmatrix}, \begin{bmatrix} 1 & 0 \\ 0 & 2 \end{bmatrix})$, $\tilde{\mathbf{x}}_2|(\tilde{y}_2 = -1) \sim \mathcal{N}(\begin{bmatrix} 5 \\ 12 \end{bmatrix}, \begin{bmatrix} 1 & 0 \\ 0 & 2 \end{bmatrix})$. We assume the probability of each sample coming out from task t is 0.5 (that is, $m_t/N \approx 0.5$ when N is large enough), for $t = 1, 2$.

We apply the single-task SVM (S-SVM), M-SVM (with different parameters) and unregularized M-SVM to the classification problems above. The excess error is summarized in Figure 2 where each dot represents the average of 2000 random experiments based on 10000 test samples. In all cases, we see

that the log-log plots of the S-SVM and M-SVM are initially parallel, then they gradually get closer and finally overlap, indicating that they have the same convergence rate but the different PCR factors. Particularly, for the similar-task case (e.g., the top left panel of Figure 2), $C_M(m_1)$ ($< C_S(m_1)$) gets smaller and approaches to $C_S(m_1)$ as the growth of λ_1 with fixed λ_2 . It is because when λ_1 becomes more significant, M-SVM makes the tasks share more information from each other. When we fix λ_1 and increase λ_2 (e.g., the top right panel), $C_M(m_1)$ ($> C_S(m_1)$) becomes smaller and gets closer to $C_S(m_1)$ in the nonsimilar-task case. This occurs because M-SVM tends to learn each task independently when λ_2 grows greatly. Moreover, in all cases, the positive or negative improvement of PCR factors in MTL is more significant when the data size is relatively small, and it vanishes when the data size goes to infinity. These observations are consistent with our theoretical result in Theorem 4, and our claims in Section III-B1 and Section III-B3.

For the unregularized M-SVM, that is the M-SVM with its regularization parameters being zero, we see that it cannot converge to the Bayes classifier in all scenarios. This is expected because, the unregularized M-SVM cannot leverage the dissimilarity of tasks, and it simply treats two different tasks as the one. This fact supports our discussions in Section III-B2.

TABLE I: M-SVM with Gaussian Kernel

Date size	200	400	800	1600	3200
EE-NRF ^a	0.0053	0.0032	0.0020	0.0012	0.0008
PPD-SF ^b (%)	10.74%	5.78%	0.26%	10.70%	4.30%

EE-NRF^a: the excess error of M-SVM without the randomness of the sampling frequency.

PPD-SF^b: the (absolute) percentage performance difference of the M-SVM with/without the randomness of the sampling frequency. We define it as the excess error difference of these two models as a percentage of the excess error of the M-SVM. The results are computed in the similar-task setting with $\lambda_1 = 20C$, $\lambda_2 = C$ ($C = 1/2$).

TABLE II: M-SVM with Linear Kernel

Date size	70	120	200	350	600
EE-NRF ^a	0.0061	0.0038	0.0023	0.0014	0.0008
PPD-SF ^b (%)	1.47%	0.48%	3.15%	4.86%	2.86%

To quantify the effects caused by the randomness of the sampling frequency in the multi-task problem, we compute the absolute percentage performance difference (in terms of the excess error) for the M-SVM with/without this randomness in Table I and Table II. We see that, in both cases, it has a small but non-negligible effect on the M-SVM's performance, and it does not change the convergence rate (as the absolute percentage differences are relatively small when the data size is large enough). This also supports our theoretical result in Theorem 4.

We also verify our claim of Section III-B3 for several other MTL frameworks, including L21, Lasso, and SRMTL (these models can be found and solved by [26]). Figure 3 again shows that these MTL methods and their single-task counterparts have the same convergence rate (the log-log plots finally overlap) but the different PCR factors (the log-log plots are initially parallel and gradually get closer). The improvement of PCR factors in

MTL is more significant when the data size is relatively small. These observations imply that our claims in Section III-B1 and Section III-B3 hold in the general MTL frameworks.

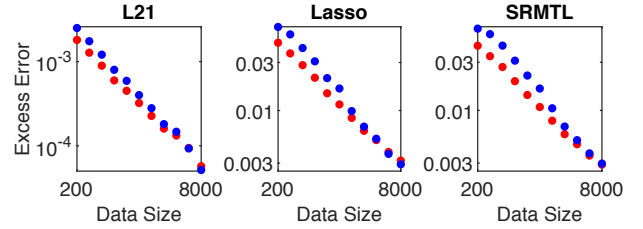


Fig. 3: Log-log plot of the excess error for the MTL methods (red) including L21, Lasso, SRMTL, and their individual counterparts (blue) in the similar-task setting. The regularization parameters for these models are 0.1, 0.4 and 0.4 (the graph regularization parameter is 0.01), respectively.

C. Experiments on blast furnace dataset

In this section, we verify our results on real blast furnace data. The dataset are collected from two typical Chinese blast furnaces with the inner volume of about 2500 m^3 and 750 m^3 , referred as blast furnace (a) and (b), respectively. Table III lists the features that are relevant for predicting the silicon class labels for these two blast furnaces. We labeled the records satisfying $(x_6 \leq 0.4132) / (x_6 \leq 0.3736)$ for furnace (a) / (b) as -1 , and $+1$ otherwise [34], [35]. Due to the (2-8h) time delay for furnace outputs to respond to inputs, we also treat 4 lagged terms for the first five features as inputs [36]. Furnaces (a) and (b) have 794 and 800 samples, respectively.

TABLE III: Input variables For blast furnaces

Variable name [Unit]	Symbol	Input variable
Blast volume [m^3/min]	x_1	$q^{-1}, q^{-2}, q^{-3}, q^{-4}$
Blast temperature [$^{\circ}\text{C}$]	x_2	$q^{-1}, q^{-2}, q^{-3}, q^{-4}$
Feed speed [mm/h]	x_3	$q^{-1}, q^{-2}, q^{-3}, q^{-4}$
Gas permeability [$\text{m}^3/\text{min}\cdot\text{kPa}$]	x_4	$q^{-1}, q^{-2}, q^{-3}, q^{-4}$
Pulverized coal injection [ton]	x_5	$q^{-1}, q^{-2}, q^{-3}, q^{-4}$
Silicon content [wt%]	x_6	q^{-1}

$q^{-1}, q^{-2}, q^{-3}, q^{-4}$ represent delay operators, e.g., $q^{-1}x(t) = x(t-1)$.

We apply the S-SVM, M-SVM (with different parameters), and unregularized M-SVM using a linear kernel to the silicon classification problems. The misclassification error (the Bayes classifier is unknown here) is summarized in Figure 4 where each dot represents the average of 10000 random splits of the datasets with $m_1 = 100, 110, 120, \dots, 490$ samples as the training set and the remaining 300 ones as the test set. For each partition, we normalize the variables of training samples to zero mean and unit variance, while the test samples are normalized accordingly. We see that the performance curves of the S-SVM and M-SVM are separable initially, then they get closer gradually and overlap finally, indicating that they have the same convergence rate but different PCR factors. Moreover, the improvement of PCR factors in MTL is more significant when the data size is relatively small. This phenomenon excellently

agrees with the results of the simulation studies above. In addition, we observe from Figure 4 that the unregularized M-SVM initially outperforms the M-SVM, due to the intrinsic similarity of these two furnaces. However, the unregularized M-SVM performs worse than the S-SVM and M-SVM when the training data size is relatively large. This occurs because the unregularized M-SVM classifier cannot converge to the corresponding Bayes rule without the regularization terms.

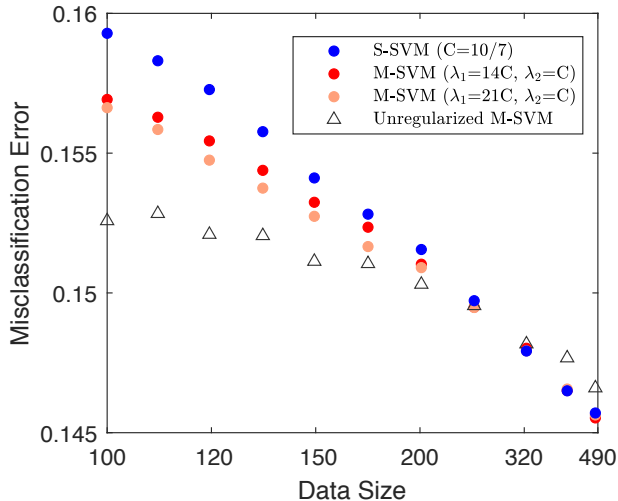


Fig. 4: This figure shows the misclassification error plots for the S-SVM, M-SVM, and unregularized M-SVM on blast furnace data. The horizontal axis is given in $1/m_1$ scale and is sorted in ascending order. We see that the plots of the S-SVM and M-SVM are initially separable, then they gradually get closer and finally overlap, indicating that they have the same convergence rate but the different PCR factors. Without the regularization terms, the unregularized M-SVM classifier cannot converge to the corresponding Bayes rule.

V. DISCUSSION

There are a number of future works we are currently pursuing related to the error analysis of the regularized MTL.

We provided both the theoretical (in a one-dimensional least-square classification setting) and experimental justification to support our claim that the benefit of MTL is the improvement the PCR factor rather than the convergence rate. Based on the theoretical results of this simple case, we also discussed the conditions under which the MTL technique originating from [19] can improve the PCR factor. It would be interesting to theoretical verify this claim in more general MTL frameworks (e.g., the MTL methods listed in introduction), which requires a more elaborate analysis of the central limit property of the learning methods. We leave this issue for future work.

Another interesting question is whether we can still get optimal asymptotic performance (i.e., Bayes risk consistency) in the MTL setting discussed in this paper by assuming there are some common structures of functional space \mathcal{H} for each task. Maurer et al. [16] considered a similar problem in the context of an unregularized MTL problem where a common feature representation of different tasks is shared. They also

derived the error upper bound for this learning method. It is unknown whether sharing a common feature representation in MTL can achieve optimal performance.

Intuitively, learning multiple tasks simultaneously in a model may interrupt the learning process of each task when we enforce the structural information to be shared between the classifiers. For example, by considering to decompose an infinite dimensional functional space \mathcal{H} into the directed sum of two sub-spaces \mathcal{H}_1 and \mathcal{H}_2 , that is $\mathcal{H} = \mathcal{H}_1 + \mathcal{H}_2$, and assuming the function f_t for each task t can be written as $f_t = f_0 + g_t$ where $f_0 \in \mathcal{H}_1$ and $g_t \in \mathcal{H}_2$, for every $t \in \{1, \dots, T\}$. In this case, the feasible space of functions for all T tasks $(f_0, g_1, g_2, \dots, g_T)$ is $\mathcal{H}_1 \times \prod_{i=1}^T \mathcal{H}_2$, rather than $\prod_{i=1}^T \mathcal{H}$ considered in Eq. (3). Thus, the classifier learned by MTL using the common functional structure technique may not converges to the Bayes rule in the limit of large data size, due to the smaller feasible functional space. The discussion indicates that it is important to balance the complexity of functional space and the computational costs in MTL.

Note that we can reformulate M-SVM (3) as a standard SVM problem with N training data [19]. If solving a SVM requires the time $\mathcal{O}(m_t^2)$ [37] for each task, the complexity of M-SVM would be $\mathcal{O}(N^2)$, where $N = \sum_{t=1}^T m_t$. Therefore, it is necessary to speedup M-SVM by using a parallelized computational structure when encountering the big data. To achieve this, we need to properly decompose the optimization problem (3) into T subproblems for the T tasks. For example, we can adapt a decomposing method from [38] to design the parallel algorithm for M-SVM. However, it is out of the scope of this work and will be left to future work.

Another attractive problem is generalizing our analysis framework to the regularized online MTL problems, where the large-scale data arrive sequentially. Especially, it is interesting to analyze the stochastic generalization error bounds in terms of the step sizes and the approximation property of functional space when the various regularization terms are included in the functional iterations to model different task relations.

VI. CONCLUSIONS

In this work, we analyze the M-SVM's asymptotic performance by focusing on the asymptotic behaviors of the learned classifier in terms of the excess misclassification error. We first generalize the regularized multi-task learning (MTL) model [19] by introducing the kernel map and the uncertainty of data frequency of tasks into it. Then, we show the upper bound of the excess misclassification error to be $\mathcal{O}((\log N)^{-s/4})$ almost surely. This result demonstrates that the regularized MTL framework can produce reliable classification rules when the sample size goes to infinity. Furthermore, we find that the interaction of tasks vanishes as the data size goes to infinity, and the convergence rates of the M-SVM and its single-task counterpart have the same upper bound. The former suggests that M-SVM cannot improve the limit classifier's performance; based on the latter fact, we raise the conjecture that the optimal convergence rate is not improved either when the number of tasks is fixed.

As a novel insight of MTL, our theoretical and experimental results achieved an excellent agreement that the benefit of M-

SVM lies in improving the pre-convergence-rate (PCR) factor (denoted as the ratio between the excess misclassification error and its real convergence rate in Section III) rather than the convergence rate. This improvement of PCR factors is more significant when the data size is small. Moreover, our simulation results of several other MTL methods, including L21, Lasso, and SRMTL (these models can be found and solved by [26]) also demonstrate the generality of this new insight in MTL. Therefore, PCR factor is more suitable and accurate to depict the essential advantages of MTL when the task number is fixed.

APPENDIX

A. Proofs

The proof of Lemma 2. Notice that

$$\mathcal{E}(f_1^z, \dots, f_T^z) - \mathcal{E}(f_1^*, \dots, f_T^*) \quad (\text{A.1})$$

$$= \{\mathcal{E}(f_1^z, \dots, f_T^z) - \mathcal{E}_z(f_1^z, \dots, f_T^z)\} \quad (\text{A.2})$$

$$+ \left\{ \mathcal{E}_z(f_1^z, \dots, f_T^z) + \frac{\rho_1}{N} \sum_{t=1}^T \frac{m_t}{N} \|f_t^z\|_K^2 + \frac{\rho_2}{N} \sum_{t=1}^T \frac{m_t}{N} \left\| f_t^z - \sum_{s=1}^T \frac{m_s}{N} f_s^z \right\|_K^2 \right\} \quad (\text{A.3})$$

$$- \left\{ \mathcal{E}_z(f_1^{\mathcal{H}}, \dots, f_T^{\mathcal{H}}) + \frac{\rho_1}{N} \sum_{t=1}^T p(t) \|f_t^{\mathcal{H}}\|_K^2 + \frac{\rho_2}{N} \sum_{t=1}^T p(t) \left\| f_t^{\mathcal{H}} - \sum_{s=1}^T p(s) f_s^{\mathcal{H}} \right\|_K^2 \right\} \quad (\text{A.4})$$

$$+ \{\mathcal{E}_z(f_1^{\mathcal{H}}, \dots, f_T^{\mathcal{H}}) - \mathcal{E}(f_1^{\mathcal{H}}, \dots, f_T^{\mathcal{H}})\} \quad (\text{A.5})$$

$$+ \left\{ \mathcal{E}(f_1^{\mathcal{H}}, \dots, f_T^{\mathcal{H}}) - \mathcal{E}(f_1^*, \dots, f_T^*) + \frac{\rho_1}{N} \sum_{t=1}^T p(t) \|f_t^{\mathcal{H}}\|_K^2 + \frac{\rho_2}{N} \sum_{t=1}^T p(t) \left\| f_t^{\mathcal{H}} - \sum_{s=1}^T p(s) f_s^{\mathcal{H}} \right\|_K^2 \right\} \quad (\text{A.6})$$

$$- \frac{\rho_1}{N} \sum_{t=1}^T \frac{m_t}{N} \|f_t^z\|_K^2 - \frac{\rho_2}{N} \sum_{t=1}^T \frac{m_t}{N} \left\| f_t^z - \sum_{s=1}^T \frac{m_s}{N} f_s^z \right\|_K^2$$

Moreover, there is

$$\begin{aligned} & (\text{A.4}) \\ & \leq - \left\{ \mathcal{E}_z(f_1^{\mathcal{H}}, \dots, f_T^{\mathcal{H}}) + \frac{\rho_1}{N} \sum_{t=1}^T \frac{m_t}{N} \|f_t^{\mathcal{H}}\|_K^2 + \frac{\rho_2}{N} \sum_{t=1}^T \frac{m_t}{N} \left\| f_t^{\mathcal{H}} - \sum_{s=1}^T \frac{m_t}{N} f_s^{\mathcal{H}} \right\|_K^2 \right\} \\ & - \frac{\rho_1}{N} \sum_{t=1}^T \left(p(t) - \frac{m_t}{N} \right) \|f_t^{\mathcal{H}}\|_K^2 \\ & + \frac{\rho_2}{N} \sum_{t=1}^T \left(\frac{m_t}{N} - p(t) \right) \left\| f_t^{\mathcal{H}} - \sum_{s=1}^T \frac{m_s}{N} f_s^{\mathcal{H}} \right\|_K^2 \\ & + \frac{2\rho_2}{N} \sum_{t=1}^T p(t) \left\| f_t^{\mathcal{H}} - \sum_{s=1}^T \frac{m_s}{N} f_s^{\mathcal{H}} \right\|_K \left\| \sum_{t=1}^T \left(p(t) - \frac{m_t}{N} \right) f_t^{\mathcal{H}} \right\|_K \end{aligned}$$

Combining above inequality with (A.3), we obtained

$$\begin{aligned} & (\text{A.3}) + (\text{A.4}) \\ & \leq - \frac{\rho_1}{N} \sum_{t=1}^T \left(p(t) - \frac{m_t}{N} \right) \|f_t^{\mathcal{H}}\|_K^2 \\ & + \frac{\rho_2}{N} \sum_{t=1}^T \left(\frac{m_t}{N} - p(t) \right) \left\| f_t^{\mathcal{H}} - \sum_{s=1}^T \frac{m_s}{N} f_s^{\mathcal{H}} \right\|_K^2 \\ & + \frac{2\rho_2}{N} \sum_{t=1}^T p(t) \left\| f_t^{\mathcal{H}} - \sum_{s=1}^T \frac{m_s}{N} f_s^{\mathcal{H}} \right\|_K \left\| \sum_{t=1}^T \left(p(t) - \frac{m_t}{N} \right) f_t^{\mathcal{H}} \right\|_K \end{aligned}$$

Denote the right hand side of above inequality as $\mathcal{F}(N, T, \rho_1, \rho_2)$, $\mathcal{S}(N, T) = (\text{A.2}) + (\text{A.5})$, and $\mathcal{D}(N, T, \rho_1, \rho_2) = (\text{A.6})$, we obtain the result. \square

Before showing the proof of Lemma 3, we first provide some auxiliary lemmas which will be helpful for the later proof. The first one bounds the minimizer of M-SVM and its average empirical loss.

Lemma A.6. For functions $\ell(\cdot)$ and f_t^z , we have

- $\sum_{i=1}^{m_t} \frac{\ell(y_{i,t} \cdot f_t^z(\mathbf{x}_{i,t}))}{m_t} \leq \frac{N}{m_t}$
- $\|f_t^z\|_K \leq \frac{N}{\sqrt{\rho_1 \cdot m_t}}$

Proof. Let's define an auxiliary function $\tilde{f}(\cdot) \equiv 0$ which obviously lies in \mathcal{H}_K . Note that $\{f_t^z\}$ minimize the objective function 3. Therefore, we have the following relation

$$\begin{aligned} & \sum_{t=1}^T \sum_{i=1}^{m_t} \ell(y_{i,t} \cdot f_t^z(\mathbf{x}_{i,t})) + \rho_1 \sum_{t=1}^T \frac{m_t}{N} \|f_t^z\|_K^2 \\ & + \rho_2 \sum_{t=1}^T \frac{m_t}{N} \left\| f_t^z - \sum_{s=1}^T \frac{m_s}{N} f_s^z \right\|_K^2 \\ & \leq \sum_{t=1}^T \sum_{i=1}^{m_t} \ell(y_{i,t} \cdot \tilde{f}(\mathbf{x}_{i,t})) + \rho_1 \sum_{t=1}^T \frac{m_t}{N} \|\tilde{f}\|_K^2 \\ & + \rho_2 \sum_{t=1}^T \frac{m_t}{N} \left\| \tilde{f} - \sum_{s=1}^T \frac{m_s}{N} \tilde{f} \right\|_K^2. \end{aligned}$$

Since the left hand side of above inequality is greater than or equals to $\sum_{i=1}^{m_t} \ell(y_{i,t} \cdot f_t^z(\mathbf{x}_{i,t}))$, where $t = 1, \dots, T$, and the right hand side of the inequality equals to N , we have the relation

$$\sum_{i=1}^{m_t} \ell(y_{i,t} \cdot f_t^z(\mathbf{x}_{i,t})) \leq N, \quad \text{and} \quad \sum_{i=1}^{m_t} \frac{\ell(y_{i,t} \cdot f_t^z(\mathbf{x}_{i,t}))}{m_t} \leq \frac{N}{m_t}.$$

Similarly, since $\rho_1 \frac{m_t}{N} \|f_t^z\|_K^2$ is also less than or equals to the left hand side of the first inequality in this lemma, therefore, we have

$$\rho_1 \frac{m_t}{N} \|f_t^z\|_K^2 \leq N, \quad \text{and} \quad \|f_t^z\|_K \leq \frac{N}{\sqrt{\rho_1 \cdot m_t}}.$$

Thus the result is shown. \square

The second auxiliary lemma bounds the sampling error as $\mathcal{O}(\frac{1}{\sqrt{N}})$.

Lemma A.7. For a sequence of bounded, independent, and identically distributed random variables $\{X_i\}$, there is

$$\frac{\sum_{i=1}^N X_i}{N} - \mathbb{E}X_1 = \mathcal{O}\left(N^{-\frac{1}{2}+\epsilon}\right) \quad \text{a.s.}$$

where ϵ is any positive constant.

Proof. It can be proven directly by applying the Borel-Cantelli lemma to the Hoeffding's inequality. \square

The third auxiliary lemma bounds the generalization error of the M-SVM classifier.

Lemma A.8.

$$\mathbb{E}_{(\mathcal{X}, \mathcal{Y}) \sim P_t} [\ell(\mathcal{Y} \cdot f_t^z(\mathcal{X}))] - \sum_{i=1}^{m_t} \frac{\ell(y_{i,t} \cdot f_t^z(\mathbf{x}_{i,t}))}{m_t} \leq \mathcal{O}\left(N^{-\frac{1}{4}+\epsilon}\right) \cdot \sum_{N=1}^{\infty} P \left\{ \tilde{\mathcal{E}}_t(f_t^z) - \tilde{\mathcal{E}}_t^z(f_t^z) > 4 \left(1 + \frac{N}{m_t}\right) \cdot \alpha^*(N, m_t) \mid m_t \right\} < +\infty.$$

Proof. We first denote some notations as follow:

$$\begin{aligned} \tilde{\mathcal{E}}_t(f) &:= \mathbb{E}_{(\mathcal{X}, \mathcal{Y}) \sim P_t} [\ell(\mathcal{Y} \cdot f_t^z(\mathcal{X}))] \\ \tilde{\mathcal{E}}_t^z(f) &:= \sum_{i=1}^{m_t} \frac{\ell(y_{i,t} \cdot f_t^z(\mathbf{x}_{i,t}))}{m_t} \\ \mathcal{B}_R &:= \{f \in \mathcal{H}_K \mid \|f\|_K \leq R\} \end{aligned}$$

Let $R^* = \frac{N}{\sqrt{\rho_1 m_t}}$, then by Lemma A.6 $f_t^z \in \mathcal{B}_{R^*}$. Together with the fact that $\tilde{\mathcal{E}}_t^z(f_z) \leq \frac{N}{m_t}$ (c.f Theorem A.6), for any $\alpha > 0$ we have

$$\begin{aligned} &P \left\{ \tilde{\mathcal{E}}_t(f_t^z) - \tilde{\mathcal{E}}_t^z(f_t^z) > 4\alpha \left(1 + \frac{N}{m_t}\right) \mid m_t \right\} \\ &\leq P \left\{ \sup_{f \in \mathcal{B}_{R^*}} \frac{\tilde{\mathcal{E}}_t(f) - \tilde{\mathcal{E}}_t^z(f)}{1 + \tilde{\mathcal{E}}_t^z(f)} > 4\alpha \mid m_t \right\} \\ &\leq \mathcal{N} \left(\frac{\alpha}{R^*} \right) \exp \left\{ -\frac{m_t \cdot \alpha^2}{32(1 + \kappa R^*)} \right\} \end{aligned} \quad (\text{A.7})$$

where the last inequality follows from lemma 5 in [20], and $\mathcal{N} \left(\frac{\alpha}{R^*} \right)$ is the covering number defined as the minimal number of balls with radius $\frac{\alpha}{R^*}$ to cover the unite ball in RKHS. According to [32], the covering number has the relation

$$\log \mathcal{N}(\epsilon) \leq M \left(\log \frac{1}{\epsilon} \right)^{d+1}$$

where M is a constant, and d is the dimension of the data set space. By plugging above inequality and $\alpha = \alpha^*(N, m_t) = N^\epsilon \cdot \sqrt{\frac{1+\kappa R^*}{m_t}}$ into (A.7), we have

$$\begin{aligned} &P \left\{ \tilde{\mathcal{E}}_t(f_t^z) - \tilde{\mathcal{E}}_t^z(f_t^z) > 4 \left(1 + \frac{N}{m_t}\right) \cdot \alpha^*(N, m_t) \mid m_t \right\} \\ &\leq \exp \left\{ M \left(\log \frac{N}{N^\epsilon \sqrt{\rho_1 + \rho_1 \kappa R^*}} \right)^{d+1} - \frac{1}{32} N^{2\epsilon} \right\} \\ &\leq \exp \left\{ M \left(\log \frac{N^{1-\epsilon}}{\sqrt{\rho_1}} \right)^{d+1} - \frac{1}{32} N^{2\epsilon} \right\} \end{aligned} \quad (\text{A.8})$$

where ϵ is arbitrary positive constant. Furthermore, by above inequality and some easy calculations we can obtain

$$\begin{aligned} &P \left\{ \tilde{\mathcal{E}}_t(f_t^z) - \tilde{\mathcal{E}}_t^z(f_t^z) > 4 \left(1 + \frac{N}{m_t}\right) \cdot \alpha^*(N, m_t) \mid m_t \right\} \\ &= \mathbb{E}_{m_t} \left[P \left\{ \tilde{\mathcal{E}}_t(f_t^z) - \tilde{\mathcal{E}}_t^z(f_t^z) > 4\alpha \left(1 + \frac{N}{m_t}\right) \mid m_t \right\} \right] \\ &\leq \mathbb{E}_{m_t} \left[\exp \left\{ M \left(\log \frac{N^{1-\epsilon}}{\sqrt{\rho_1}} \right)^{d+1} - \frac{1}{32} N^{2\epsilon} \right\} \right] \\ &= o(N^{-2}), \end{aligned}$$

and, therefore,

By Borel-Cantelli Lemma, we have the relation

$$\limsup_{N \rightarrow \infty} \tilde{\mathcal{E}}_t(f_t^z) - \tilde{\mathcal{E}}_t^z(f_t^z) - 4 \left(1 + \frac{N}{m_t}\right) \cdot \alpha^*(N, m_t) \leq 0 \quad \text{a.s.}$$

Besides, according to the definition of $\alpha^*(\cdot, \cdot)$ and the strong law of large numbers, we have $\left(1 + \frac{N}{m_t}\right) \cdot \alpha^*(N, m_t) = \mathcal{O}(N^{-1/4+\epsilon})$. Thus, $\tilde{\mathcal{E}}_t(f_t^z) - \tilde{\mathcal{E}}_t^z(f_t^z) \leq \mathcal{O}(N^{-1/4+\epsilon})$ which proves the result. \square

With these preparations, we can prove Lemma 3.

The proof of Lemma 3. We first consider the first part of sample error, $\mathcal{E}(f_1^z, \dots, f_T^z) - \mathcal{E}_z(f_1^z, \dots, f_T^z)$. By the definition and some easy calculations, we can obtain,

$$\begin{aligned} &\mathcal{E}(f_1^z, \dots, f_T^z) - \mathcal{E}_z(f_1^z, \dots, f_T^z) \\ &= \sum_{t=1}^T p(t) \left(\mathbb{E}_{(\mathcal{X}, \mathcal{Y}) \sim P_t} [\ell(\mathcal{Y} \cdot f_t^z(\mathcal{X}))] - \sum_{i=1}^{m_t} \frac{\ell(y_{i,t} \cdot f_t^z(\mathbf{x}_{i,t}))}{m_t} \right) \\ &\quad + \sum_{t=1}^T \left[\left(p(t) - \frac{m_t}{N} \right) \sum_{i=1}^{m_t} \frac{\ell(y_{i,t} \cdot f_t^z(\mathbf{x}_{i,t}))}{m_t} \right] \end{aligned} \quad (\text{A.9})$$

Since, for each task t , the random variable m_t is a counting process with bounded and independent increments, therefore, by Lemma A.7, there holds

$$p(t) - \frac{m_t}{N} = \mathbb{E} \left(\frac{m_t}{N} \right) - \frac{m_t}{N} = \mathcal{O}\left(N^{-\frac{1}{2}+\epsilon}\right) \quad \text{a.s.} \quad (\text{A.10})$$

By plugging above relation and lemma A.8 into (A.9), this relation leads to

$$\mathcal{E}(f_1^z, \dots, f_T^z) - \mathcal{E}_z(f_1^z, \dots, f_T^z) = \mathcal{O}\left(N^{-\frac{1}{4}+\epsilon}\right) \quad \text{a.s.} \quad (\text{A.11})$$

Then we consider the second part of sample error, $\mathcal{E}_z(f_1^{\mathcal{H}}, \dots, f_T^{\mathcal{H}}) - \mathcal{E}(f_1^{\mathcal{H}}, \dots, f_T^{\mathcal{H}})$. Still by the definition and some easy calculations, we can obtain,

$$\begin{aligned} & \mathcal{E}_z(f_1^{\mathcal{H}}, \dots, f_T^{\mathcal{H}}) - \mathcal{E}(f_1^{\mathcal{H}}, \dots, f_T^{\mathcal{H}}) \\ &= \sum_{t=1}^T \left[\left(\frac{m_t}{N} - p(t) \right) \sum_{i=1}^{m_t} \frac{\ell(y_{i,t} \cdot f_t^{\mathcal{H}}(\mathbf{x}_{i,t}))}{m_t} \right] \\ & \quad + \sum_{t=1}^T p(t) \left[\sum_{i=1}^{m_t} \frac{\ell(y_{i,t} \cdot f_t^{\mathcal{H}}(\mathbf{x}_{i,t}))}{m_t} \right] \\ & \quad - \mathbb{E}_{(\mathcal{X}, \mathcal{Y}) \sim P_t} [\ell(\mathcal{Y} \cdot f_t^{\mathcal{H}}(\mathcal{X}))] \end{aligned} \quad (\text{A.12})$$

Moreover, since $\ell(y_{i,t} \cdot f_t^{\mathcal{H}}(\mathbf{x}_{i,t})) = \max\{0, 1 - y_{i,t} f_t^{\mathcal{H}}(\mathbf{x}_{i,t})\} \leq 1 + \|f_t^{\mathcal{H}}\|_{\infty} \leq 1 + \kappa \|f_t^{\mathcal{H}}\|_K$ and $\|f_t^{\mathcal{H}}\|_K$ is finite, for each data sample $\ell(y_{i,t} \cdot f_t^{\mathcal{H}}(\mathbf{x}_{i,t}))$ is uniformly bounded by a constant R where $R = 1 + \kappa \|f_t^{\mathcal{H}}\|_K$. Therefore, by (A.10) and the uniform boundedness of $\ell(y_{i,t} \cdot f_t^{\mathcal{H}}(\mathbf{x}_{i,t}))$, there holds

$$\begin{aligned} & \sum_{t=1}^T \left[\left(\frac{m_t}{N} - p(t) \right) \sum_{i=1}^{m_t} \frac{\ell(y_{i,t} \cdot f_t^{\mathcal{H}}(\mathbf{x}_{i,t}))}{m_t} \right] \\ & \leq \sum_{t=1}^T \left[\left(\frac{m_t}{N} - p(t) \right) \sum_{i=1}^{m_t} \frac{R}{m_t} \right] = \mathcal{O}\left(N^{-\frac{1}{2}+\epsilon}\right) \quad \text{a.s.} \end{aligned} \quad (\text{A.13})$$

Besides, due to i.i.d. property of sampled data $(\mathbf{x}_{i,t}, y_{i,t})$ for each task t , the random variable $\ell(y_{i,t} \cdot f_t^{\mathcal{H}}(\mathbf{x}_{i,t}))$ is also independent and identically distributed. Together with the boundedness of $\ell(y_{i,t} \cdot f_t^{\mathcal{H}}(\mathbf{x}_{i,t}))$, we can apply *Lemma A.7* to $\ell(y_{i,t} \cdot f_t^{\mathcal{H}}(\mathbf{x}_{i,t}))$ and obtain $\sum_{i=1}^{m_t} \frac{\ell(y_{i,t} \cdot f_t^{\mathcal{H}}(\mathbf{x}_{i,t}))}{m_t} - \mathbb{E}_{(\mathcal{X}, \mathcal{Y}) \sim P_t} [\ell(\mathcal{Y} \cdot f_t^{\mathcal{H}}(\mathcal{X}))] = \mathcal{O}\left(N^{-\frac{1}{2}+\epsilon}\right)$ a.s.. By plugging this equation and (A.13) into the last two lines of (A.12), we obtain

$$\mathcal{E}_z(f_1^{\mathcal{H}}, \dots, f_T^{\mathcal{H}}) - \mathcal{E}(f_1^{\mathcal{H}}, \dots, f_T^{\mathcal{H}}) = \mathcal{O}\left(N^{-\frac{1}{2}+\epsilon}\right) \quad \text{a.s.} \quad (\text{A.14})$$

Finally combining (A.11) and (A.14), we have $\mathcal{S}(N, T) = \mathcal{O}\left(N^{-\frac{1}{4}+\epsilon}\right)$ a.s., which proves this lemma. \square

The proof of Lemma 4. First, we note that function $\ell(x) = \max\{0, 1-x\}$ is a Lipschitz function, satisfying $|\ell(x) - \ell(y)| \leq |x - y|$ where x and y are arbitrary real numbers. Therefore, for any $h_1, h_2, \dots, h_T \in \mathcal{H}_K$ there is

$$\begin{aligned} & \mathcal{E}(h_1, \dots, h_T) - \mathcal{E}(f_1^*, \dots, f_T^*) \\ & \leq \sum_{i=1}^T p(t) \mathbb{E}_{(\mathcal{X}, \mathcal{Y}) \sim P_t} |h_t(\mathcal{X}) - f_t^*(\mathcal{X})| \\ & \leq \sum_{i=1}^T p(t) \left(\mathbb{E}_{(\mathcal{X}, \mathcal{Y}) \sim P_t} |h_t(\mathcal{X}) - f_t^*(\mathcal{X})|^2 \right)^{1/2} \end{aligned}$$

where the first inequality follows from Lipschitz continuity and the second one follows from Holder inequality. For simplicity, we denote $\|h_t - f_t\|_{\mathcal{L}_{P_t}^2} :=$

$\left(\mathbb{E}_{(\mathcal{X}, \mathcal{Y}) \sim P_t} |h_t(\mathcal{X}) - f_t^*(\mathcal{X})|^2 \right)^{1/2}$. Through plugging above the last inequality to $D(N, T, \rho_1, \rho_2)$, we have

$$\begin{aligned} & D(N, T, \rho_1, \rho_2) \\ & \leq \inf_{h_1, \dots, h_T \in \mathcal{H}_K} \left\{ \sum_{t=1}^T p(t) \|h_t - f_t^*\|_{\mathcal{L}_{P_t}^2} + \frac{\rho_1}{N} \sum_{t=1}^T p(t) \|f_t^*\|_K^2 \right. \\ & \quad \left. + \frac{\rho_2}{N} \sum_{t=1}^T p(t) \left\| h_t - \sum_{s=1}^T p(s) h_s \right\|_K^2 \right\} \\ & \leq \inf_{R>0} \left\{ \inf_{\substack{h_1, \dots, h_T \in \mathcal{H}_K \\ \|h_t\|_K \leq R}} \left\{ \sum_{t=1}^T p(t) \|h_t - f_t^*\|_{\mathcal{L}_{P_t}^2} \right\} \right. \\ & \quad \left. + \frac{\rho_1 R^2}{N} + \frac{2\rho_2 R^2}{N} \right\} \\ & \leq \inf_{R>0} \left\{ C_0 C_s (\log R)^{-s/4} + \frac{\rho_1 R^2}{N} + \frac{2\rho_2 R^2}{N} \right\} \end{aligned}$$

where the last inequality follows immediately from [33], [39]. In above, C_0 and s are two positive constants, while C_s is another constant depends on s . By choosing $R = N^{1/2-\epsilon}$ where $\epsilon > 0$, we have $D(N, T, \rho_1, \rho_2) \leq C_0 C_s ((1/2 - \epsilon) \log N)^{-s/4} + \rho_1 N^{-\epsilon} + 2\rho_2 N^{-\epsilon} = \mathcal{O}(\log N)^{-s/4}$, which proves the result. \square

The proof of Lemma 5. By the definition and some easy calculation, we get

$$\begin{aligned} & \mathcal{F}(N, T, \rho_1, \rho_2) \\ & \leq -\frac{\rho_1}{N} \sum_{i=1}^T \left(p(t) - \frac{m_t}{N} \right) \|f_t^{\mathcal{H}}\|_K^2 \\ & \quad + \frac{\rho_2}{N} \sum_{t=1}^T \left\| p(t) - \frac{m_t}{N} \right\| \left(\|f_t^{\mathcal{H}}\|_K + \sum_{s=1}^T \|f_s^{\mathcal{H}}\|_K \right)^2 \\ & \quad + \frac{2\rho_2}{N} \left(\sum_{t=1}^T \left\| p(t) - \frac{m_t}{N} \right\| \cdot \|f_t^{\mathcal{H}}\|_K \right) \\ & \quad \times \left(\sum_{t=1}^T \|f_t^{\mathcal{H}}\|_K + \sum_{s=1}^T \|f_s^{\mathcal{H}}\|_K \right) \end{aligned}$$

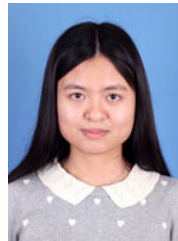
where the terms $\frac{\rho_1}{N}$, $\frac{\rho_2}{N}$, and $p(t) - \frac{m_t}{N}$ determine the convergent rate of the frequency error. Since, for each task t , the random variable m_t is a counting process with bounded and independent increments, therefore, by *Lemma A.7*, there holds $p(t) - \frac{m_t}{N} = \mathbb{E}\left(\frac{m_t}{N}\right) - \frac{m_t}{N} = \mathcal{O}\left(N^{-\frac{1}{2}+\epsilon}\right)$ a.s..

Therefore, $\mathcal{F}(T, N, \rho_1, \rho_2) \leq \mathcal{O}\left(N^{-\frac{3}{2}+\epsilon}\right)$ a.s., which shows the result. \square

REFERENCES

- [1] R. Caruana, "Multitask learning," *Machine learning*, vol. 28, no. 1, pp. 41–75, 1997.
- [2] Y. Chen, S. Song, S. Li, L. Yang, and C. Wu, "Domain space transfer extreme learning machine for domain adaptation," *IEEE transactions on cybernetics*, vol. 49, no. 5, pp. 1909–1922, 2018.
- [3] D. Li, Z. Gong, and D. Zhang, "A common topic transfer learning model for crossing city poi recommendations," *IEEE transactions on cybernetics*, vol. 49, no. 12, pp. 4282–4295, 2018.

- [4] D. Wang, C. Lu, J. Wu, H. Liu, W. Zhang, F. Zhuang, and H. Zhang, "Softly associative transfer learning for cross-domain classification," *IEEE transactions on cybernetics*, vol. 50, no. 11, pp. 4709–4721, 2019.
- [5] J. Wang, Q. Wang, H. Zhang, J. Chen, S. Wang, and D. Shen, "Sparse multiview task-centralized ensemble learning for asd diagnosis based on age-and sex-related functional connectivity patterns," *IEEE transactions on cybernetics*, vol. 49, no. 8, pp. 3141–3154, 2018.
- [6] X. Gu, F.-L. Chung, H. Ishibuchi, and S. Wang, "Multitask coupled logistic regression and its fast implementation for large multitask datasets," *IEEE transactions on cybernetics*, vol. 45, no. 9, pp. 1953–1966, 2014.
- [7] Y. Jiang, Z. Deng, F.-L. Chung, and S. Wang, "Multi-task fuzzy system modeling using inter-task correlation information," *Information Sciences*, vol. 298, pp. 512–533, 2015.
- [8] Y. Jiang, Z. Deng, K.-S. Choi, F.-L. Chung, and S. Wang, "A novel multi-task fuzzy classifier and its enhanced version for labeling-risk-aware multi-task classification," *Information Sciences*, vol. 357, pp. 39–60, 2016.
- [9] T. Evgeniou, C. A. Micchelli, M. Pontil, and J. Shawe-Taylor, "Learning multiple tasks with kernel methods," *Journal of machine learning research*, vol. 6, no. 4, 2005.
- [10] K. Yu, V. Tresp, and A. Schwaighofer, "Learning gaussian processes from multiple tasks," in *Proceedings of the 22nd international conference on Machine learning*, pp. 1012–1019, 2005.
- [11] Y. Zhang and Q. Yang, "A survey on multi-task learning," *IEEE Transactions on Knowledge and Data Engineering*, 2021.
- [12] R. K. Ando, T. Zhang, and P. Bartlett, "A framework for learning predictive structures from multiple tasks and unlabeled data," *Journal of Machine Learning Research*, vol. 6, no. 11, 2005.
- [13] J. Baxter, "Learning internal representations," in *Proceedings of the eighth annual conference on Computational learning theory*, pp. 311–320, 1995.
- [14] J. Baxter, "A model of inductive bias learning," *Journal of artificial intelligence research*, vol. 12, pp. 149–198, 2000.
- [15] J. Baxter, "A bayesian/information theoretic model of learning to learn via multiple task sampling," *Machine learning*, vol. 28, no. 1, pp. 7–39, 1997.
- [16] A. Maurer, M. Pontil, and B. Romera-Paredes, "The benefit of multitask representation learning," *Journal of Machine Learning Research*, vol. 17, no. 81, pp. 1–32, 2016.
- [17] T. Liu, D. Tao, M. Song, and S. J. Maybank, "Algorithm-dependent generalization bounds for multi-task learning," *IEEE transactions on pattern analysis and machine intelligence*, vol. 39, no. 2, pp. 227–241, 2016.
- [18] C. Zhang, D. Tao, T. Hu, and B. Liu, "Generalization bounds of multitask learning from perspective of vector-valued function learning," *IEEE Transactions on Neural Networks and Learning Systems*, vol. 32, no. 5, pp. 1906–1919, 2020.
- [19] T. Evgeniou and M. Pontil, "Regularized multi-task learning," in *Proceedings of the tenth ACM SIGKDD international conference on Knowledge discovery and data mining*, pp. 109–117, 2004.
- [20] Q. Wu and D.-X. Zhou, "Analysis of support vector machine classification," *Journal of Computational Analysis & Applications*, vol. 8, no. 2, 2006.
- [21] D.-R. Chen, Q. Wu, Y. Ying, and D.-X. Zhou, "Support vector machine soft margin classifiers: error analysis," *The Journal of Machine Learning Research*, vol. 5, pp. 1143–1175, 2004.
- [22] Y. Ying and D.-X. Zhou, "Online regularized classification algorithms," *IEEE Transactions on Information Theory*, vol. 52, no. 11, pp. 4775–4788, 2006.
- [23] Y. Ying and D.-X. Zhou, "Learnability of gaussians with flexible variances," 2007.
- [24] J. Lin, L. Rosasco, and D.-X. Zhou, "Iterative regularization for learning with convex loss functions," *The Journal of Machine Learning Research*, vol. 17, no. 1, pp. 2718–2755, 2016.
- [25] Y. Fan, S. Lyu, Y. Ying, and B.-G. Hu, "Learning with average top-k loss," *arXiv preprint arXiv:1705.08826*, 2017.
- [26] J. Zhou, J. Chen, and J. Ye, "Malsar: Multi-task learning via structural regularization," *Arizona State University*, vol. 21, 2011.
- [27] L. Devroye, L. Györfi, and G. Lugosi, *A probabilistic theory of pattern recognition*, vol. 31. Springer Science & Business Media, 2013.
- [28] I. Steinwart and A. Christmann, *Support vector machines*. Springer Science & Business Media, 2008.
- [29] Q. Wu, Y. Ying, and D.-X. Zhou, "Multi-kernel regularized classifiers," *Journal of Complexity*, vol. 23, no. 1, pp. 108–134, 2007.
- [30] Y. Lin, Y. Lee, and G. Wahba, "Support vector machines for classification in nonstandard situations," *Machine learning*, vol. 46, no. 1, pp. 191–202, 2002.
- [31] T. Zhang, "Statistical behavior and consistency of classification methods based on convex risk minimization," *The Annals of Statistics*, vol. 32, no. 1, pp. 56–85, 2004.
- [32] D.-X. Zhou, "The covering number in learning theory," *Journal of Complexity*, vol. 18, no. 3, pp. 739–767, 2002.
- [33] D.-X. Zhou, "Density problem and approximation error in learning theory," in *Abstract and Applied Analysis*, vol. 2013, Hindawi, 2003.
- [34] S. Chen and C. Gao, "Linear priors mined and integrated for transparency of blast furnace black-box svm model," *IEEE Transactions on Industrial Informatics*, vol. 16, no. 6, pp. 3862–3870, 2019.
- [35] C. Gao, Q. Ge, and L. Jian, "Rule extraction from fuzzy-based blast furnace svm multiclassifier for decision-making," *IEEE Transactions on Fuzzy Systems*, vol. 22, no. 3, pp. 586–596, 2013.
- [36] S. Chen, N. V. Sahinidis, and C. Gao, "Transfer learning in information criteria-based feature selection," *arXiv preprint arXiv:2107.02847*, 2021.
- [37] C.-C. Chang and C.-J. Lin, "Libsvm: a library for support vector machines," *ACM transactions on intelligent systems and technology (TIST)*, vol. 2, no. 3, pp. 1–27, 2011.
- [38] Y. Zhang, "Parallel multi-task learning," in *2015 IEEE International Conference on Data Mining*, pp. 629–638, IEEE, 2015.
- [39] S. Smale and D.-X. Zhou, "Estimating the approximation error in learning theory," *Analysis and Applications*, vol. 1, no. 01, pp. 17–41, 2003.



Shaohan Chen received the B.Sc. degrees in Mathematics and Applied Mathematics from Jimei University, China, in 2014. She is currently working towards the Ph.D. degree in operational research and cybernetics at Zhejiang University.

Her research interests are in the areas of machine learning models design and interpretations.



Zhou Fang received the B.Sc. and Ph.D. degrees in mathematics from Zhejiang university, China, in 2014 and 2019, respectively. Since November 2019, he has been a postdoc with the department of biosystems science and engineering, at ETH-Zürich, Switzerland.

His research interests are in the areas of learning theory, control theory, and systems/synthetic biology.



Sijie Lu received the B.Sc. degrees in Mathematics from China agricultural university, China, in 2019. She is currently working towards the MS.C. degree in operational research and cybernetics at Zhejiang University. Her research interests are in the areas of machine learning and its industrial applications.



Chuanhou Gao received the B.Sc. degrees in chemical engineering from Zhejiang University of Technology, China, in 1998, and the Ph.D. degrees in operational research and cybernetics from Zhejiang University, China, in 2004. From June 2004 until May 2006, he was a Postdoctor in the Department of Control Science and Engineering at Zhejiang University. Since June 2006, he has been with the Department of Mathematics at Zhejiang University, where he is currently a full Professor. His research interests are in the areas of data-driven modeling,

control and optimization, problems-driven applied mathematics, machine learning and transparency of black-box modeling techniques.

Dr. Gao was a Guest Editor of IEEE TRANSACTIONS ON INDUSTRIAL INFORMATICS, ISIJ International and Journal of Applied Mathematics and an editor of Metallurgical Industry Automation from May 2013. Currently, he is an associate editor of IEEE Transactions on Automatic Control.